Lasers in Manufacturing Conference 2019

Hot Electron Plasma Temperatures and Soft X-Ray Emission During Laser Processing with Ultrafast Lasers

Rudolf Weber[a*], Roswitha Giedl-Wagner[b], Daniel Förster[a,c], Thomas Graf[a], Anton Pauli[b]

[a]*Institut für Strahlwerkzeuge (IFSW), Universität Stuttgart, Pfaffenwaldring 43, 70569 Stuttgart, Germany*
[b]*GFH GmbH, Großwalding 5, 94469 Deggendorf, Germany*
[c]*LighPulse Laser Precision, Pfaffenwaldring 43, 70569 Stuttgart, Germany*

Abstract

Soft X-ray emission during industrial materials processing with ultrafast lasers is of increasing interest. The soft X-rays mainly originate from the free, hot electrons in the plasma. Therefore, the spectrum of the emission approximately follows a Maxwell-Boltzmann distribution, which corresponds to the temperature of the hot electrons.
For the current work, the spectra of the soft X-ray emission were measured for intensities between about 10^{13} W/cm^2 and 10^{15} W/cm^2. The corresponding temperatures of the hot electrons were determined by fitting Maxwell-Boltzmann distributions to the spectra. Furthermore, the resulting H(0.07) dose rates at a distance of 20 cm from the plasma were measured and extrapolated to dose rates for an average laser power of 1 kW.

Keywords: Laser plasma, soft X-ray emission, dose rates, Ultrafast laser processing, hot-electron temperature temperature

1. Introduction

Materials processing with ultra-short laser pulses below about 10 ps at high irradiances > 10^{10} W/cm^2 is very promising for achieving perfect quality as e.g. described by Nolte et al. (1997), Hügel et. al. (1998), and Schultz et. al. (2013).

* Corresponding author. Tel.: +49-711-685-66844;
E-mail address: rudolf.weber@ifsw.uni-stuttgart.de .

However, during the interaction of intense laser pulses with metals, X-ray emission is generated. X-ray emission from laser-produced plasma in vacuum has been investigated since the early 1980ies, as e.g. described in Corkum et. al. (1988), Lampart et. al. (1988), and Weber et. al. (1988). X-rays emitted from laser-induced plasma were used, in particular, in indirect driven fusion and X-ray laser research, later also for X-ray lithography and x-ray spectroscopy.

The process leading to X-ray emission is described in detail by Giulietti et. al. (1998) where it can be seen that the X-ray emission for photon energies > 1 keV is mainly created by Bremsstrahlung and recombination emission from the hot electrons in the plasma.

Today, X-ray emission during industrial laser processing, i.e. in ambient pressure at high average powers might become an issue as published by Legall et. al. (2918) and Behrens et. al. (2018), where extensive measurement of the dose rates resulting from materials processing with ps-laser pulses is presented. The actual German radiation protection ordinance defines 50 mSv per year as limiting value.

The major reason for the increasing importance of this issue is that the average power of ultrafast lasers is continuously increasing, from typically 100 W today to well above 1 kW as demonstrated by Negel et. al. (2013) and Müller et. al. (2018). In this proceeding, measurements of the hot-electron temperatures and H(0.07) dose rates during processing of steel are presented for the range of irradiances of about 10^{11} W/cm^2 to 10^{15} W/cm^2, which is relevant for industrial processing. In addition, an extrapolation of the measured dose rates to an average laser power of 1 kW is presented.

2. Measured spectra

Fig. 1. shows the emission spectra, which was measured with a silicon-drift detector (PNDetector GmbH, Munich, Germany) as a function of the photon energy. The measurements were made through air at atmospheric pressure at a distance of 13.5 cm (left) and 20 cm (right). The sample material was tungsten. The laser provided pulses with a duration of 0.9 ps (left) and 0.24 ps (right). The laser pulse energy was 0.18 mJ, the repetition rate 100 kHz, and the beam was focused onto the surface of the sample to a focus diameter of 45 µm in both cases. This resulted in irradiances I_0 of $2.6 \cdot 10^{13}$ W/cm^2 (left) and $9.8 \cdot 10^{13}$ W/cm^2 (right). The irradiance I_0 is given by

$$I_0 = \frac{2 \cdot E_P}{t_P \cdot \pi \cdot r_F^2} \tag{1}$$

where E_p is the laser pulse energy, t_p the pulse duration and r_F the laser spot radius on the surface.

$I_0 = 2.6 \cdot 10^{13}$ W/cm^2 $I_0 = 9.8 \cdot 10^{13}$ W/cm^2

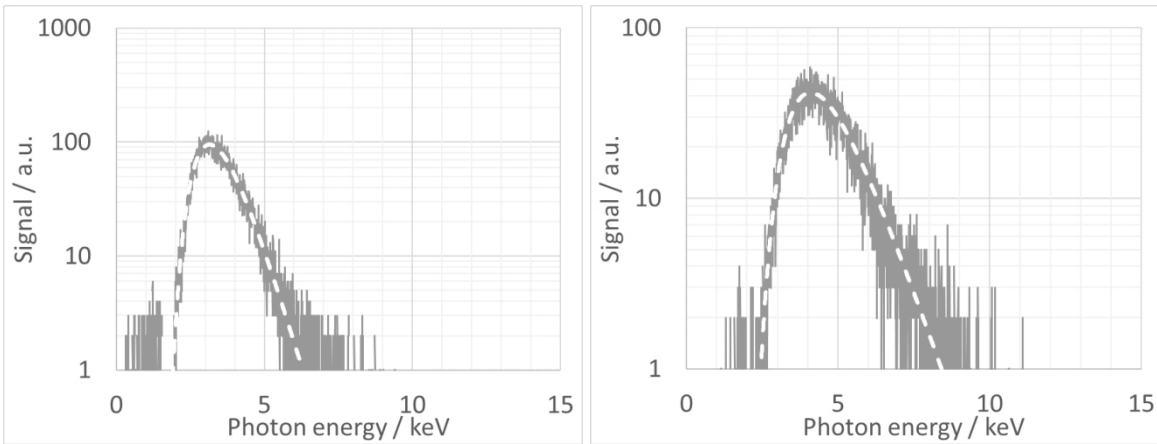

Fig. 1. Spectra of the thermal Bremsstrahlung from tungsten plasma generated by a laser with a wavelength of 1 µm, with a pulse duration of 0.9 ps, and an irradiance I_0 of $2.6 \cdot 10^{13}$ W/cm^2 (left), and with a pulse duration of 0.24 ps and an irradiance I_0 of $9.8 \cdot 10^{13}$ W/cm^2 (right). The dashed white lines are fits using eq. (2), which yield a temperature of 0.45 keV (left) and of 0.82 keV (right).

Following the theory of Giulietti et. al. (1998) the spectrum of the emitted Bremsstrahlung can be described by

$$S_X(\omega) = T_{tot}(\omega) \cdot c_X \cdot e^{-\frac{\hbar \cdot \omega}{k_B \cdot T_h}} \tag{2}$$

Where $T_{tot}(\omega)$ is the total, frequency-dependent transmission trough air and all filters in the detector. T_h is the hot-electron temperature, k_B and $\hbar$ the Boltzmann and Planck constant, respectively. c_X is a frequency-independent constant which was used to scale the calculated to the measured spectra. The white dashed lines in Fig. 1. represent fits to the spectra using eq. (2). The only fit-parameter is the hot-electron temperature T_h. For the two fits shown in Fig. 1. the resulting temperature is 0.48 keV (left) and 0.82 keV (right).

3. Hot-electron temperatures

Fig 2. shows the hot-electron temperature as a function of the irradiance multiplied by the laser wavelength in micrometers squared, as determined from the measured spectra for different setups. The dashed line represents the temperature scaling as given by Tan et.al. (1984). It is noted, that the lowest irradiance considered in Tan et. al. (1984) was 10^{14} W/cm^2. The dash-dotted line represents a least-square power fit to the measured data. The error bars correspond to $\pm 15\%$ which was estimated from applying fits with different T_h. The scaling constants are labelled in the graph.

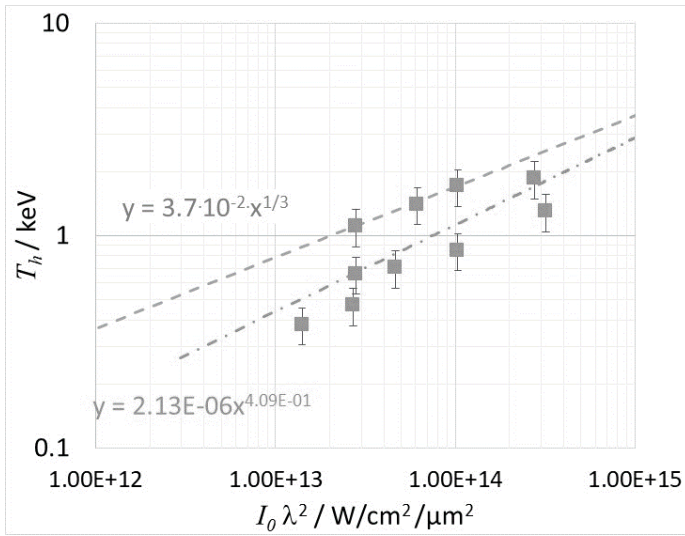

Fig. 2. Measured hot-electron temperatures for different setups. The dashed line represents the temperature scaling as given by Tan et.al. (1984). The dash-dotted line represents a least-square power fit to the measured data.

It is seen, that most of the measured temperatures are below the values predicted by fit given in Tan et. al. (1984). Furthermore, the temperature seems to decrease stronger with decreasing $I_0 \cdot \lambda^2$ than expected from the scaling in Tan et. al. (1984).

4. Dose conversion

In addition to the spectra, the H(0.07) dose rates were measured at GFH GmbH with OD-02 dosimeters (STEP GmbH, Pockau, Germany) at a distance of 20 cm from the plasma. The used laser had a wavelength of 1.03 µm, a pulse duration of 921 fs, a constant repetition rate of 300 kHz, and a maximum pulse energy of 346 µJ, yielding a maximum average power of 104 W. For the experiments, the laser spot was scanned over a small area of 20 mm x 20 mm on the surface of the steel sample in order to prevent shielding from remaining material around the emission area. The line overlap and the pulse overlap were kept constant at about 75%. The irradiance I_0 was changed by changing the pulse energy. As the pulse energy changed, also the average laser power increases with increasing irradiance. Therefore, the measured dose rates were normalized with the average power yielding the dose in µSv per µJ of pulse energy ("dose conversion efficiency for a distance of 20 cm through air", η_{Dose20}). The resulting dose per pulse energy is shown as dots in Fig. 3. The error bars were estimated from the scattering of the data points achieved with different setups not included here. The solid line is the fit to the data using a model by Weber et. al. (1019) which is based on Gulietti et. al. (1998).

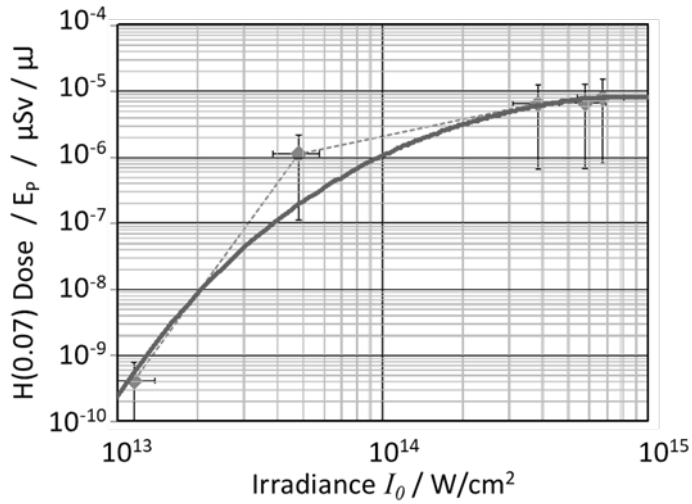

Fig. 3. H(0.07) dose per pulse energy at a distance of 20 cm from the interaction zone, referred to as η_{Dose20} in the text, as a function of the irradiance I_0. The dots represent the normalized measured dose rates, the solid line a mode-fit to the data.

The strong decrease of the dose conversion efficiency between 10^{14} W/cm^2 and 10^{13} W/cm^2 confirms the measured steeper decrease of the hot-electron temperature below 10^{14} W/cm^2.

5. Scaling and shielding

The fit to the dose conversion efficiency η_{Dose20} in Fig. 3. (left) was used to calculate the expected H(0.07) dose rate at a distance of 20 cm from the plasma for a constant average power of 104 W as was the maximum average power of the GFH-system (Fig. 4. (left), solid line). In the calculation the irradiance was increased by decreasing the laser spot size. In addition, the expected H(0.07) dose rate was calculated for an average laser power of 1 kW. The expected dose rate simply increases linear with increasing laser power. It is seen that at 1 kW the H(0.07) dose rate is about 25'000 µSv/h at the irradiance about $2.2 \cdot 10^{13}$ W/cm^2. This means that the limit of 25 mSv for one year is reached after one hour.

Although this is apparently a large value, it must be noted that this only holds for the maximum measurable emisson from the surface without any material shielding and in the very close distance of 20 cm to the plasma. Furthermore it can be seen from Fig. 1. (left) that almost the complete spectrum lays below the critical photon energy of 5 keV where the OD-02 might still be sensitive. Furthermore, the optimum irradiance for ps-laser processing with respect to both, quality and efficiency is about 5-10 times above threshold. For a pulse duration of 1 ps and iron this is at an effective irradiance of about 10^{11} W/cm^2, which is far below the critical $2.2 \cdot 10^{13}$ W/cm^2. The effective irradiance accounts for the angle of incidence and the size of the processed structures such as holes or grooves.

Fig. 4. (right) shows the same calculated emission but including the attenuation of a filter of 2 mm thick steel plate between the plasma and the detector. With this 2 mm steel shielding the expected dose rates are well below 1 µSv/h at the irradiance of $1 \cdot 10^{13}$ W/cm^2, which means well below any critical value.

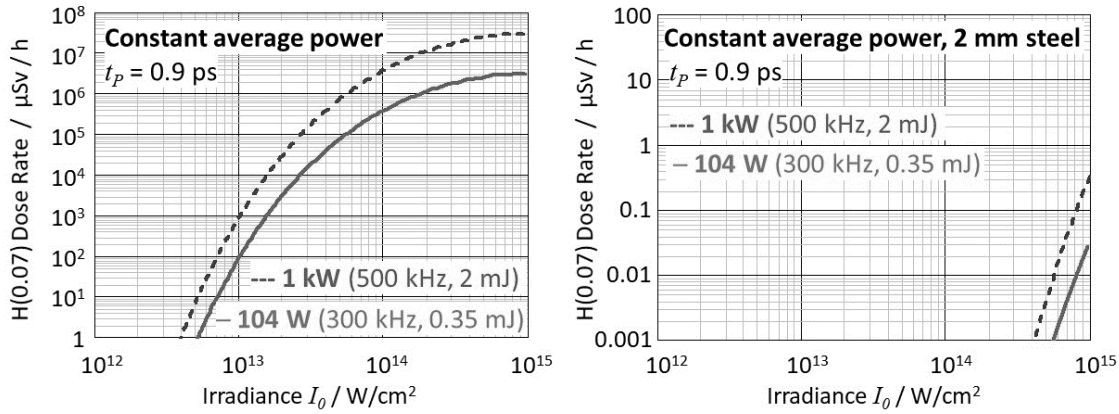

Fig. 4. (left) Expected H(0.07) dose rates for 104 W and 1 kW of constant average laser power as a function of the irradiance at a distance of 20 cm from the plasma. The intensity increased by decreasing the laser spot size. (right) The dose achieved with the same processing parameters but with an additional filter of 2 mm steel between the plasma and the detector.

6. Summary

The measured hot-electron temperatures show a stronger decrease below 10^{14} W/cm^2 than expected from the scaling law published by Tan et.al. (1984). This is confirmed by the strong decrease of the H(0.07) dose conversion efficiency η_{Dose20} between 10^{14} W/cm^2 and 10^{13} W/cm^2. Nevertheless, the annual dose limit of 25 mSv can be reached after one hour when processing with 1 kW of average power at about $2.2 \cdot 10^{13}$ W/cm^2.

However, under normal processing conditions such as the optimum effective fluence of about 10^{11} W/cm^2 and usual laser safety with a metal housing in a distance of at least half a meter from the plasma the X-ray emission is no issue. If processing at effective irradiances > 10^{13} W/cm^2 is required for some reason, shielding with about 2 mm of steel is recommended and safe according to the above findings.

7. Acknowledgement

This work was funded in parts by the BMBF in the frame of the project Sculp^{3}T

8. References

S. Nolte, C. Momma, H. Jacobs, A. Tünnermann, B. N. Chichkov, B. Wellegehausen, and H. Welling, “Ablation of metals by ultrashort laser pulses,” J. Opt. Soc. Am. B, 14 (10) (1997).

H. Hügel, H. Schittenhelm, K. Jasper, G. Callies, and P. Berger, “Structuring with excimer lasers - experimental and theoretical investigations on quality and efficiency,” J. Laser Appl. 10 (1998).

W. Schulz, U. Eppelt, and R. Poprawe, “Review on laser drilling I. Fundamentals, modeling, and simulation”, Journal of Laser Applications 25 (1) (2013).

P.B. Corkum, F. Brunel, N.K. Sherman, T. Srinivasan-Rao, "Thermal Response of Metals to Ultrashort-Pulse Laser Excitation", Phys. Rev. Lett 61 (25), 2886-2889 (1988).

W. Lampart, R. Weber, and J. E. Balmer, „Comparative x-ray spectroscopy of various-Z elements with wavelength calibration", J. Appl. Phys. 63, 273 (1988).

R. Weber, P. F. Cunningham, J. E. Balmer, „Temporal and spectral characteristics of soft x radiation from laser-irradiated cylindrical cavities" Appl. Phys. Lett. 53 (26), (1988).

D. Giulietti, L. A. Gizzi, "X-Ray Emission from Laser Produced Plasma", La Rivista del Nuovo Cimento, 21 (10), 1 (1998)

H. Legall et al, “X-ray emission as a potential hazard during ultrashort pulse laser material processing", Applied Physics A 124, 407 (2018).

R. Behrens, B. Pullner, M. Reginatto, "X-Ray Emission From Materials Processing Lasers", Radiation Protection Dosimetry 2018, 1–14 (2018).

J. E. Balmer, T.P. Donaldson, "Resonance Absorption of 1.06-µm Laser Radiation in Laser-Generated Plasma", Phys. Rev. Lett. 17 (39), 1084 (1977).

J.-P. Negel, A. Voss, M. Abdou Ahmed, D. Bauer, D. Sutter, A. Killi, and T. Graf, “1.1 kW average output power from a thin-disk multipass amplifier for ultrashort laser pulses,” Optics Letters 38, (24), 5442-5445 (2013).

M. Müller, A. Klenke, A. Steinkopff, H. Stark, A. Tünnermann, A. Limpert, "3.5 kW coherently combined ultrafast fiber laser", Optics Letters 43(24), 6037-6040 (2018).

H. G. Tan, G. H. McCall, A. H. Williams, "Determination of laser intensity and hot electron temperature from fastest ion velocity measurement in laser-produce plasmas", Phys. Fluids 27 (1), 296 (1984).

R. Weber, R. Giedl-Wagner, D. J. Förster, A. Pauli, T. Graf, J. E. Balmer, " Expected X-ray Dose Rates Resulting from Industrial Ultrafast Laser Applications", submitted to Applied Physics A (2019)